remote sensing

MDPI

Article

Superior $PM_{2.5}$ Estimation by Integrating Aerosol Fine Mode Data from the Himawari-8 Satellite in Deep and Classical Machine Learning Models

Zhou Zang [1], Dan Li [1], Yushan Guo [1], Wenzhong Shi [2] and Xing Yan [1,*]

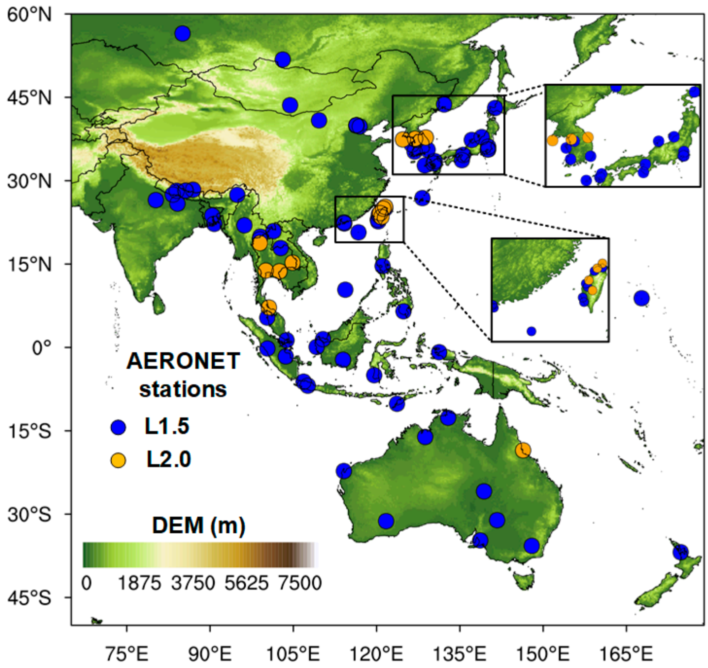

Figure S1. Map of Himawari-8/AHI imaging zone with the base map showing the DEM in meters. Blue and orange dots represent Level 1.5 (L1.5) and Level 2.0 (L2.0) AERONET stations that were used in validation, respectively.

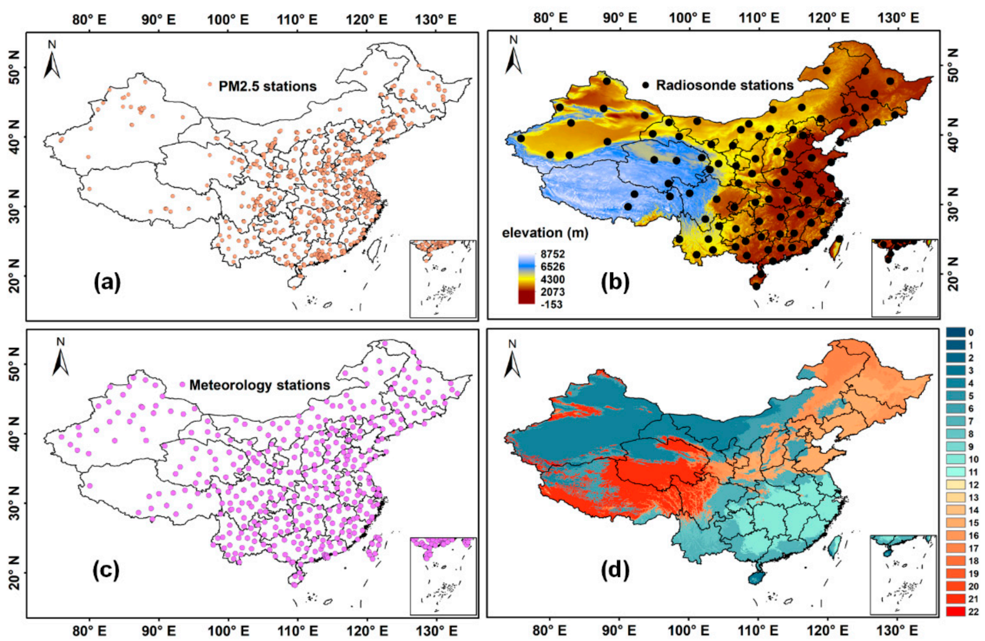

Figure S2. The study area (China) for PM2.5 estimation and the ground-level stations of **a**) 1701 PM2.5 stations (pink scatters), **b**) 95 radiosonde stations (black scatters) and the DEM over China,

c) 405 meteorology stations (magenta scatters) and **d**) climate zones over China classified by Kop-pen-Geiger climate classifications. A detailed description of the legend is shown in Table S3.

Figure S3a and S3b shows the differences in the R and RMSE values (by the V3.0 result minus the V2.0 result) for AE. This indicates that R is increased at 70.5% of stations, and RMSE is increased at 100% of stations. Stations over northern China and Japan show a particular increase in R of over 0.1 and a decrease in RMSE of over 0.2. After quality control, more stations showed increased R values (73.8%), but some stations over south-eastern Asia showed increased RMSE values ranging from 0 to 0.36. However, according to the R and RMSE values stations for V3.0 and V2.1 with AE and AE QA (Figure S4), both the V3.0 AE and V3.0 AE QA data outperformed the V2.1 data, and more stations showed high R values (> 0.15) and low RMSE values (< 0.40). This result reveals that both before and after quality control, V3.0 AE always performed better than V2.1 AE.

With respect to V3.0 and V2.1 FMF, Figure 3e and 3f show that although R was decreased at many stations over southeastern Asia, South Korea, and northern China, the RMSE was much lower at most stations (95.1%) with V3.0 FMF. As shown in Figure S5, both V2.1 and V3.0 FMF were high R (> 0.20) in northern China and Japan, and the RMSE of V3.0 FMF was particularly low (< 0.20). This result illustrates that the results of V3.0 FMF are generally better than V2.0 FMF over sites.

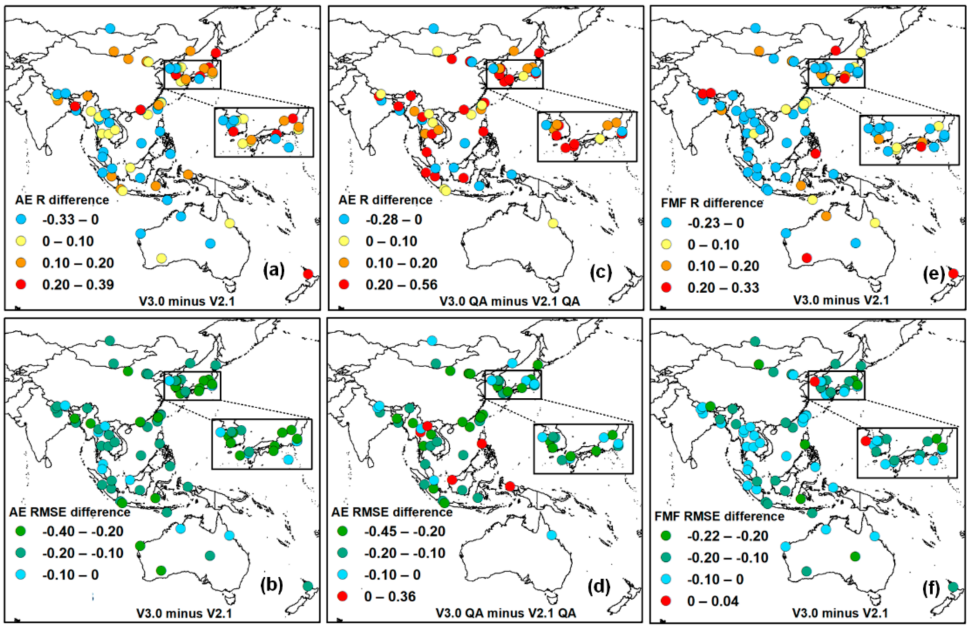

Figure S3. Differences between validation results (R and RMSE) for Himwari-8 V3.0 and V2.1 (V3.0 minus V2.1) data over AERONET sites: (**a**, **b**) for AE; (**c**, **d**) for AE after quality control (AE QA); and (**e, f**) for FMF.

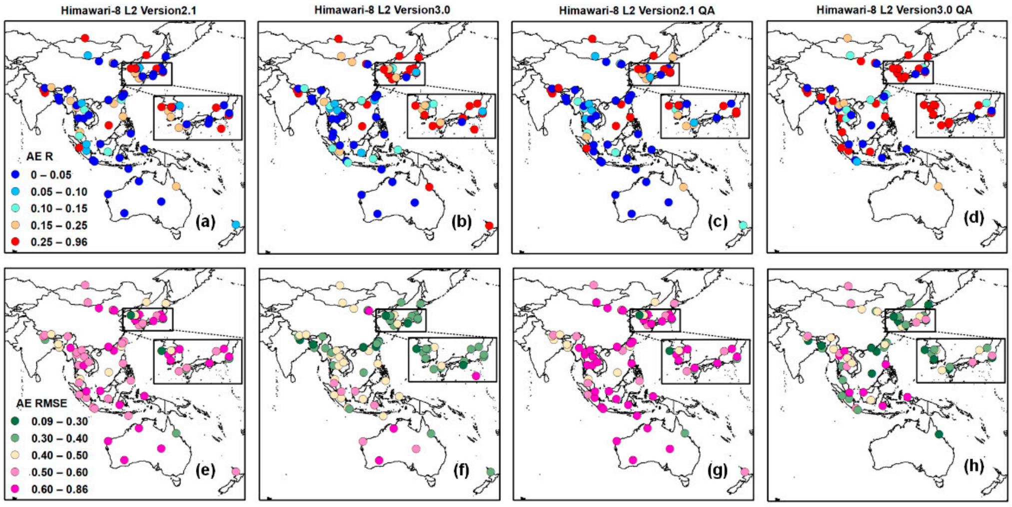

Figure S4. Validation results (R and RMSE) for Himwari-8 V3.0 and V2.1 AE over AEROENT sites: (**a**, **e**) for V2.1 AE; (**b**, **f**) for V3.0 AE; (**c**, **g**) for V2.1 AE QA; (**d**, **h**) for V3.0 AE QA.

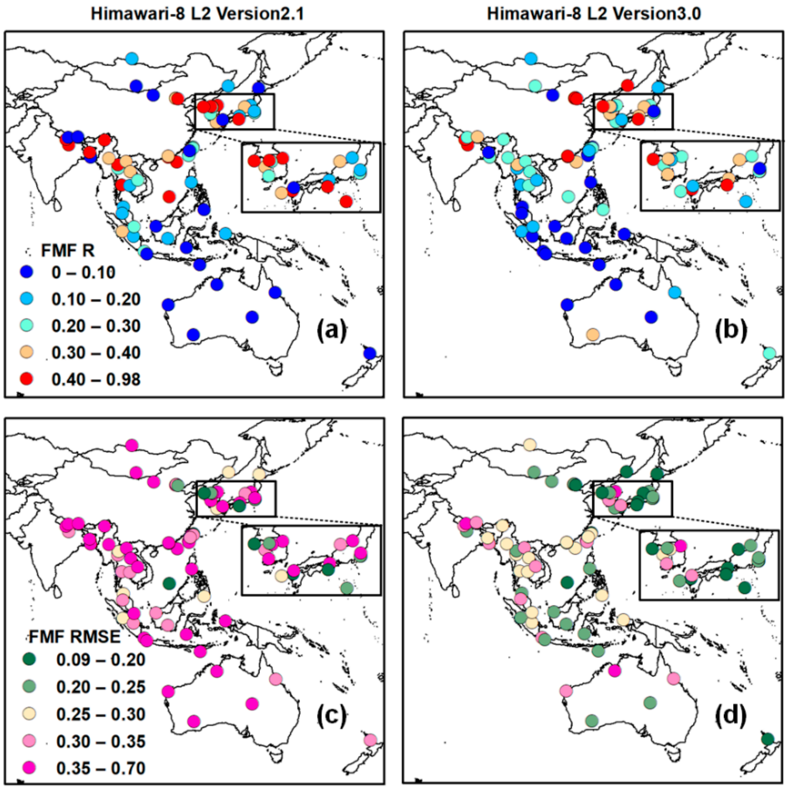

Figure S5. Validation results (R and RMSE) for Himwari-8 V3.0 and V2.1 FMF over AEROENT sites: (**a**, **c**) for V2.1 FMF; (**b**, **d**) for V3.0 FMF.

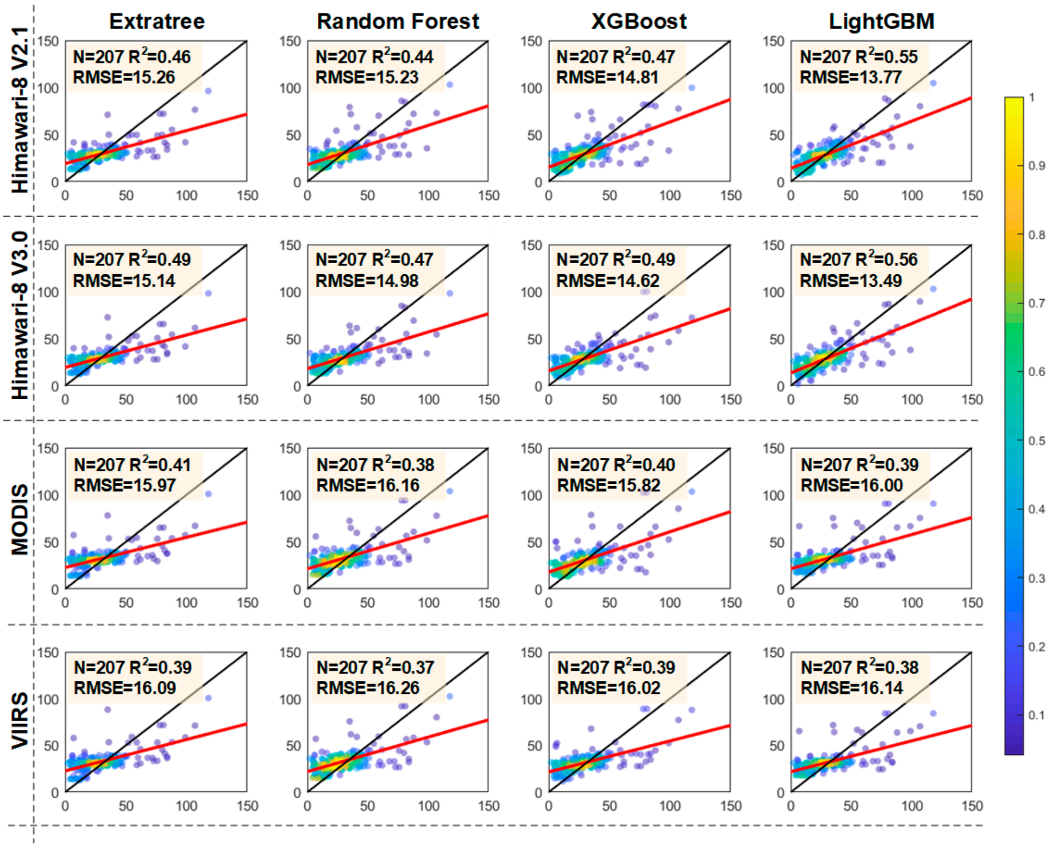

Figure S6. Density scatter plots of modeling results of ground-based $PM_{2.5}$ retrieved by four machine learning models (Extratree, Random Forest, LightGBM and XGBoost) based on four different FMF products (Himawari-8 V2.1 and V3.0 FMF, MODIS and VIIRS FMF) with the same lengths for training and test datasets. The black and red lines represent 1:1 and fitting lines, respectively. Because the amount of training data is small (N=1321), which is unsuitable for applying deep learning models, EntityDenseNet was not used for $PM_{2.5}$ estimations here.

Table S1. Previous studies of machine learning retrieved $PM_{2.5}$ since 2014.

Author	Region	Models	AOT	Aerosol size information
Chen et al. [1]	China	Random forest (RF), self-adaptive deep neural network (DNN)	Yes	No
Chen et al. [2]	Yangtze River Delta (YRD)	RF, Gradient Boosting Regression (GBR), K-nearest neighbor (KNN) regression	Yes	No
Chen et al. [3]	China	A stacking model based on AdaBoost, XGBoost, RF	Yes	No
Chen et al. [4]	United states	A two-stage model based on a multiple regression model (MRM) and an aerosol classification model (ACM)	Yes	No
Chen et al. [5]	Shenzhen	Linear regression (LR), geographically and temporally weighted regression (GTWR), RF, improved RF	Yes	No
Chen et al. [6]	China	RF, XGBoost, support vector machine (SVM), gradient boost	Yes	No

		model (GBM), generalized additive model (GAM), Bayesian regularized neural network (BRNN), least absolute shrinkage and selection operator (LASSO)		
Chu and Bilal [7]	Taiwan	Integrated GTWR, RANdom SAmple Consensus (RANSAC)	Yes	No
Di et al. [8]	United states	Ensemble model integrating GBM, RF and Neural Network (NN)	Yes	No
Dong et al. [9]	China	RF, back propagation algorithm (BPNN)	Yes	No
Fan et al. [10]	Beijing	XGBoost, Geographically Weighted Regression (GWR), Spatially Local XGBoost (SL-XGB)	Yes	No
Fang et al. [11]	China	Timely structure adaptive modeling (TSAM)	Yes	No
Feng et al. [12]	China	A ST-stacking model that combined XGBoost, k-nearest neighbour (KNN), BPNN in level 1 and LR for integration in level 2	Yes	No
Fu et al. [13]	Beijing	Mixed-effect (ME) model	Yes	No
Guo et al. [14]	China	RF	Yes	No
Han and Tong [15]	Chengdu	Improved linear mixed effect (LME) model	Yes	No
Han et al. [16]	Beijing	LME model	Yes	No
He and Christakos [17]	Beijing-Tianjin-Hebei (BTH)	A synthetic modeling framework based on the integration of (a) the Bayesian maximum entropy method that assimilates auxiliary information from land-use regression (LUR) and artificial neural network (ANN) model and (b) a space-time projection technique	Yes	No
Hu et al. [18]	East China	Spatiotemporal regression kriging (STRK) model	Yes	No
Huang et al. [19]	Hebei	LME model	Yes	No
Hung et al. [20]	New York State	Multiple linear regression (MLR), ANN	Yes	No
Imani [21]	Tehran	Proposed DNN	Yes	No
Jiang et al. [22]	China	Two-stage RF	Yes	No
Jung et al. [23]	Tehran	A proposed DNN	Yes	No
Kianian et al. [24]	United states	Lattice kriging, RF	Yes	No
Kim et al. [25]	Seoul	MLR	Yes	No
Knibbs et al. [26]	Australia	LUR	Yes	No

Kow et al. [27]	Taiwan	CNN-BP engaging a Convolutional Neural Network (CNN) and BPNN	Yes	No
Lee et al. [28]	California	LUR	Yes	No
Li et al. [29]	Iraq and Kuwait	A 4-stage model based on RF, GAM, ME	Yes	No
Li et al. [30]	China	Space-time random forest (STRF)	Yes	No
Li et al. [31]	California	An autoencoder-based full residual deep network	Yes	No
Li [32]	BTH	bootstrap aggregating (bagging) of autoencoder-based residual deep networks,	Yes	No
Li et al. [33]	Shandong	Constrained mixed-effect bagging model	Yes	No
Li et al. [34]	Eastern mainland China	Three-step residual variance constraint method (RVCM)	yes	No
Li et al. [35]	China	Geographically and temporally weighted neural network (GTWNN)	Yes	No
Li et al. [36]	China	Spatialtemporally correlated deep belief network (Geoi-DBN)	Yes	No
Li and Zhang [37]	BTH	RSRF that integrates RF and AOD	Yes	No
Li et al. [38]	Three roadside stations in Hong kong	RF, Boost Regression Trees (BRT), SVM, XGBoost, GAM, Cubist	Yes	No
Liang et al. [39]	China		Yes	No
Liu et al. [40]	China	Ensemble ML	No, using TOA instead	No
Lu et al. [41]	China	RF	Yes	No
Luo et al. [42]	Typical regions in China	A hybrid model based on BPNN and e-support vector regression (e-SVR)	Yes	No
Lv et al. [43]	BTH		Yes	No
Lyu et al. [44]	China	General linear model, fully connected NN, RD, GBM	Yes	No
Ma et al. [45]	Guangdong	Transferred bi-directional long short-term memory (TL-BLSTM)	Yes	No
Ma et al. [46]	YRD	LME	Yes	No
Nabavi et al. [47]	Tehran	RF, GBM, SVM, Multivariate Adaptive Regression Splines (MARS)	Yes	No
Nguyen et al. [48]	Vietnam	Statistically-significant regression model	Yes	No
Ni et al. [49]	BTH	BPNN	Yes	No
Park et al. [50]	Full coverage of the Geostationary Ocean Color Imager (GOCI)	RF	yes	No

Park et al. [51]	South Korea	RF	Yes	No
Park et al. [52]	United States	CNN	Yes	No
Pu and Yoo [53]	New York state	Multistage model based on GBM, quantile regression forests (QRF), RF, GBM, feed-forward DNN	Yes	No
Ren et al. [54]	United States	LM, Ridge Regression, LASSO, Elastic Net Regularization (ELASTICNET), Principal Component Regression model (PCR), Partial Least Squares Regression model (PLSR), KNN, SVR, BPNN, DNN, Regression Trees (RT), RF, XGBoost	Yes	No
Schneider et al. [55]	Great Britain	A multi-stage satellite-based machine learning model based on RF	Yes	No
Song et al. [56]	Pearl River Delta (PRD)	GWR	Yes	No
Stafoggia et al. [57]	Italy	A five-stage machine-learning approach based on RF	Yes	No
Sun et al. [58]	BTH	DNN	Yes	No
Tang et al. [59]	YRD	A two-stage RF	Yes	No
Tian et al. [60]	PRD	BPNN, Elman Neural Network (ENN), RF, Gradient Boosting Regression Tree (GBRT), SVM, GAM	Yes	No
Tong et al. [61]	Southeast region of the United States	Bidirectional LSTM Recurrent Neural Network (RNN)	Yes	No
van Donkelaar et al. [62]	North America	GWR	Yes	No
Wang et al. [63]	Wuhan Urban Agglomeration	Geo-intelligent LSTM (Geoi-LSTM)	No, using TOA instead	No
Wang et al. [64]	BTH	LME	Yes	No
Wang et al. [65]	BTH	LME	Yes	No
Wang and Sun [66]	BTH	DNN	Yes	No
Wei et al. [67]	China	Space-time extratrees (STET)	Yes	No
Wei et al. [68]	China	STET	Yes	No
Wei et al. [69]	China	STRF	Yes	No
Wu et al. [70]	BTH	Time fixed effects regression model	Yes	No
Xiao et al. [71]	BTH	Weighted long short-term memory neural network extended model (WLSTME)	Yes	No
Xiao et al. [72]	Mainland China	Bayesian Maximum Entropy (BME)-GWR	Yes	No
Xie et al. [73]	Beijing	ME model	Yes	No
Xing et al. [74]	Beijing	Temperature-based deep belief network (TDBN)	Yes	No

Xu et al. [75]	BTH	The site prediction model (TSRT)	Yes	No
Xu and Zhang [76]	Beijing	Corrected regression	Yes	No
Xu et al. [77]	British Columbia	Cubist, RF, XGBoost	Yes	No
Xue et al. [78]	China	Spatiotemporally Weighted RF (SWRF) model	Yes	No
Xue et al. [79]	BTH	LME model	Yes	No
Xue et al. [80]	Central and eastern China	Geographically and temporally weighted regression (IGTWR)	Yes	No
Yan et al. [81]	China	Spatial-Temporal Interpretable Deep Learning Model (SIDLM)	Yes	No
Yang et al. [82]	Beijing, Harbin, Xi'an, Wuhan, Chengdu, Hangzhou, Guangzhou	Cascade RF	Yes	No
Yang et al. [83]	Coastal region of China	A two-stage statistical model combing LME and SVR	Yes	No
Yang et al. [84]	Fuzhou	ME model	Yes	No
Yang et al. [85]	Zhejiang	LUR	Yes	No
You et al. [86]	China	GWR	Yes	No
You et al. [87]	China	GWR	Yes	No
Zhai et al. [88]	BTH	Best subsets regression (BSR) enhanced principal component analysis-GWR (PCA-GWR)	Yes	No
Zhan et al. [89]	China	Geographically-Weighted Gradient Boosting Machine (GW-GBM)	Yes	No
Zhang et al. [90]	Three districts in Lanzhou	A hybrid model (MTD–CNN–GRU)	Yes	No
Zhang et al. [91]	YRD	Two RF submodels	Yes	No
Zhang et al. [92]	Wuhan, Beijing, Shanghai	LME	Yes	No
Zhang et al. [93]	China	Semi-physical GWR	Yes	No
Zhang et al. [94]	China	GBDT	Yes	No
Zhang and Hu [95]	BTH	ME model	Yes	No
Zhang et al. [96]	BTH	MLR, GWR, LME	Yes	No
Zhao et al. [97]	BTH	RF	Yes	No
Zheng et al. [98]	Beijing	CNN-RF	Yes	No
Zhou et al. [99]	YRD	dynamic directed spatio-temporal graph convolution networks (DD-STGCN), LSTM, GC-LSTM, spatio-temporal graph convolution networks (STGCN)	Yes	No
Zou et al. [100]	BTH	GAM	Yes	No
Zou et al. [101]	BTH	GWR	Yes	No

Table S2. AERONET stations and their data level used in this study.

AEROENT station	Longitude	Latitude	Levels
Adelaide_Site_7	138.66	-34.73	1.5

American_Samoa	-170.56	-14.25	1.5
Anmyon	126.33	36.54	1.5
AOE_Baotou	109.63	40.85	1.5
ARIAKE_TOWER	130.27	33.10	1.5
Bandung	107.61	-6.89	1.5
Bangkok	100.52	13.75	2.0
Beijing	116.38	39.98	1.5
Beijing_RADI	116.38	40.00	1.5
Beijing-CAMS	116.32	39.93	1.5
Bhola	90.76	22.23	1.5
Bidur	85.14	27.90	1.5
Birdsville	139.35	-25.90	1.5
BMKG_GAW_PALU	120.18	-1.65	2.0
BMKG_Jakarta	106.84	-6.16	1.5
Bukit_Kototabang	100.32	-0.20	1.5
Cape_Fuguei_Station	121.54	25.30	2.0
Chen-Kung_Univ	120.20	22.99	1.5
Chiang_Dao	98.96	19.45	1.5
Chiang_Mai_Met_Sta	98.97	18.77	2.0
Chiba_University	140.10	35.62	1.5
Dalanzadgad	104.42	43.58	1.5
Dhaka_University	90.40	23.73	1.5
Dibrugarh_Univ	94.90	27.45	1.5
Doi_Ang_Khang	99.05	19.93	1.5
Dongsha_Island	116.73	20.70	1.5
Douliu	120.54	23.71	1.5
EPA-NCU	121.19	24.97	2.0
Erlin	120.41	23.93	1.5
Fowlers_Gap	141.70	-31.09	1.5
Fukue	128.68	32.75	1.5
Fukuoka	130.48	33.52	1.5
Gandhi_College	84.13	25.87	1.5
Gangneung_WNU	128.87	37.77	2.0
Gwangju_GIST	126.84	35.23	1.5
Hankuk_UFS	127.27	37.34	1.5
Hokkaido_University	141.34	43.08	1.5
Hong_Kong_PolyU	114.18	22.30	1.5
Hong_Kong_Sheung	114.12	22.48	1.5
Irkutsk	103.09	51.80	1.5
Jabiru	132.89	-12.66	1.5
Jambi	103.64	-1.63	1.5
Kanpur	80.23	26.51	1.5
Kaohsiung	120.29	22.68	1.5
Kemigawa_Offshore	140.02	35.61	1.5
KORUS_UNIST_Ulsan	129.19	35.58	1.5
Kuching	110.35	1.49	1.5
Kupang	123.67	-10.14	1.5
Kwajalein_Atoll	167.74	8.85	1.5
Kyanjin_Gompa	85.57	28.21	1.5
Lake_Argyle	128.75	-16.11	1.5
Lake_Lefroy	121.71	-31.26	1.5
Langtang_BC	85.61	28.21	1.5
Learmonth	114.10	-22.24	1.5

Luang_Namtha	101.42	20.93	1.5
Lucinda	146.39	-18.52	2.0
Lulin	120.87	23.47	2.0
Lumbini_North	83.28	27.50	1.5
Makassar	119.57	-5.00	1.5
Mandalay_MTU	96.19	21.97	1.5
Manila_Observatory	121.08	14.64	1.5
ND_Marbel_Univ	124.84	6.50	1.5
Niigata	138.94	37.85	1.5
Nong_Khai	102.72	17.88	1.5
Noto	137.14	37.33	1.5
NSPO_Taiwan	121.00	24.78	1.5
Okinawa_Hedo	128.25	26.87	1.5
Osaka	135.59	34.65	1.5
Palangkaraya	113.95	-2.23	1.5
Pokhara	83.98	28.19	1.5
Pontianak	109.19	0.08	1.5
QOMS_CAS	86.95	28.37	1.5
Seoul_SNU	126.95	37.46	1.5
Shirahama	135.36	33.69	1.5
Silpakorn_Univ	100.04	13.82	2.0
Singapore	103.78	1.30	1.5
Socheongcho	124.74	37.42	2.0
Songkhla_Met_Sta	100.60	7.18	2.0
Sorong	131.27	-0.87	1.5
Sra_Kaeo	102.50	13.69	2.0
Tai_Ping	114.36	10.38	1.5
Taipei_CWB	121.54	25.01	1.5
TGF_Tsukuba	140.10	36.11	1.5
Tomsk	85.05	56.48	1.5
Tumbarumba	147.95	-35.71	1.5
Ubon_Ratchathani	104.87	15.25	2.0
Univ_of_Auckland	174.77	-36.85	1.5
USM_Penang	100.30	5.36	1.5
Ussuriysk	132.16	43.70	1.5
XiangHe	116.96	39.75	1.5
Xitun	120.62	24.16	2.0
Yonsei_University	126.93	37.56	2.0

Table S3. The parameters for the four machine learning models used in this study.

Models	Max_depth	N_estimators	N_jobs	Learning rate
Extratrees	7	200	4	0.1
Random Forest	6	200	4	0.1
XGBoost	5	160	4	0.1
LightGBM	5	300	4	0.1

Table S4. The class types and their abbreviations of global climate zone.

Value	Abbreviation	Class type
1	Af	Tropical, rainforest
2	Am	Tropical, monsoon
3	Aw	Tropical, savannah
4	BWk	Arid, desert, cold

5	BSh	Arid, steppe, hot
6	BSk	Arid, steppe, cold
7	Cwa	Temperate, dry winter, hot summer
8	Cwb	Temperate, dry winter, warm summer
9	Cwc	Temperate, dry winter, cold summer
10	Cfa	Temperate, no dry season, hot summer
11	Cfb	Temperate, no dry season, warm summer
12	Cfc	Temperate, no dry season, cold summer
13	Dsb	Cold, dry summer, warm summer
14	Dsc	Cold, dry summer, cold summer
15	Dwa	Cold, dry winter, hot summer
16	Dwb	Cold, dry winter, warm summer
17	Dwc	Cold, dry winter, cold summer
18	Dfa	Cold, no dry season, hot summer
19	Dfb	Cold, no dry season, warm summer
20	Dfc	Cold, no dry season, cold summer
21	ET	Polar, tundra
22	EF	Polar, frost

Table S5. The evaluation of MODIS, VIIRS and Himawari-8 V2.1 and V3.0 FMF against the AERONET stations mainland China.

Products	RMSE	R	N
MODIS	0.53	0.30	272
VIIRS	0.55	0.31	430
Himawari-8 V2.1	0.37	0.21	8959
Himawari-8 V3.0	0.21	0.54	7378

Reference

1. Chen, B., Lin, Y., Deng, J., Li, Z., Dong, L., Huang, Y., & Wang, K. (2021a). Spatiotemporal dynamics and exposure analysis of daily PM2.5 using a remote sensing-based machine learning model and multi-time meteorological parameters. Atmospheric Pollution Research, 12, 23-31
2. Chen, B., You, S., Ye, Y., Fu, Y., Ye, Z., Deng, J., Wang, K., & Hong, Y. (2021b). An interpretable self-adaptive deep neural network for estimating daily spatially-continuous PM2.5 concentrations across China. The Science of the total environment, 768, 144724-144724
3. Chen, J., Yin, J., Zang, L., Zhang, T., & Zhao, M. (2019a). Stacking machine learning model for estimating hourly PM2.5 in China based on Himawari 8 aerosol optical depth data. Science of the Total Environment, 697
4. Chen, Q.-X., Huang, C.-L., Yuan, Y., Mao, Q.-J., & Tan, H.-P. (2019b). Assessment of aerosol types on improving the estimation of surface PM2.5 concentrations by using ground-based aerosol optical depth dataset. Atmospheric Pollution Research, 10, 1843-1851
5. Chen, W., Ran, H., Cao, X., Wang, J., Teng, D., Chen, J., & Zheng, X. (2020a). Estimating PM2.5 with high-resolution 1-km AOD data and an improved machine learning model over Shenzhen, China. Science of the Total Environment, 746
6. Chen, Z.-Y., Jin, J.-Q., Zhang, R., Zhang, T.-H., Chen, J.-J., Yang, J., Ou, C.-Q., & Guo, Y. (2020b). Comparison of Different Missing-Imputation Methods for MAIAC (Multiangle Implementation of Atmospheric Correction) AOD in Estimating Daily PM2.5 Levels. Remote Sensing, 12
7. Chu, H.-J., & Bilal, M. (2019). PM2.5 mapping using integrated geographically temporally weighted regression (GTWR) and random sample consensus (RANSAC) models. Environmental Science and Pollution Research, 26, 1902-1910
8. Di, Q., Amini, H., Shi, L., Kloog, I., Silvern, R., Kelly, J., Sabath, M.B., Choirat, C., Koutrakis, P., Lyapustin, A., Wang, Y., Mickley, L.J., & Schwartz, J. (2019). An ensemble-based model of PM2.5 concentration across the contiguous United States with high spatiotemporal resolution. Environment International, 130
9. Dong, L., Li, S., Yang, J., Shi, W., & Zhang, L. (2020). Investigating the performance of satellite-based models in estimating the surface PM2.5 over China. Chemosphere, 256
10. Fan, Z., Zhan, Q., Yang, C., Liu, H., & Bilal, M. (2020). Estimating PM2.5 Concentrations Using Spatially Local Xgboost Based on Full-Covered SARA AOD at the Urban Scale. Remote Sensing, 12
11. Fang, X., Zou, B., Liu, X., Sternberg, T., & Zhai, L. (2016). Satellite-based ground PM2.5 estimation using timely structure adaptive modeling. Remote Sensing of Environment, 186, 152-163

12. Feng, L., Li, Y., Wang, Y., & Du, Q. (2020). Estimating hourly and continuous ground-level PM2.5 concentrations using an ensemble learning algorithm: The ST-stacking model. Atmospheric Environment, 223
13. Fu, D., Xia, X., Duan, M., Zhang, X., Li, X., Wang, J., & Liu, J. (2018). Mapping nighttime PM2.5 from VIIRS DNB using a linear mixed-effect model. Atmospheric Environment, 178, 214-222
14. Guo, B., Zhang, D., Pei, L., Su, Y., Wang, X., Bian, Y., Zhang, D., Yao, W., Zhou, Z., & Guo, L. (2021). Estimating PM2.5 concentrations via random forest method using satellite, auxiliary, and ground-level station dataset at multiple temporal scales across China in 2017. The Science of the total environment, 778, 146288-146288
15. Han, W., & Tong, L. (2019). Satellite-Based Estimation of Daily Ground-Level PM2.5 Concentrations over Urban Agglomeration of Chengdu Plain. Atmosphere, 10
16. Han, W., Tong, L., Chen, Y., Li, R., Yan, B., & Liu, X. (2018). Estimation of High-Resolution Daily Ground-Level PM2.5 Concentration in Beijing 2013-2017 Using 1 km MAIAC AOT Data. Applied Sciences-Basel, 8
17. He, J., & Christakos, G. (2018). Space-time PM2.5 mapping in the severe haze region of Jing-Jin-Ji (China) using a synthetic approach. Environmental Pollution, 240, 319-329
18. Hu, H., Hu, Z., Zhong, K., Xu, J., Zhang, F., Zhao, Y., & Wu, P. (2019). Satellite-based high-resolution mapping of ground-level PM2.5 concentrations over East China using a spatiotemporal regression kriging model. Science of the Total Environment, 672, 479-490
19. Huang, Y., Ji, Y., Zhu, Z., Zhang, T., Gong, W., Xia, X., Sun, H., Zhong, X., Zhou, X., & Chen, D. (2020). Satellite-based spatiotemporal trends of ambient PM2.5 concentrations and influential factors in Hubei, Central China. Atmospheric Research, 241
20. Hung, W.-T., Lu, C.-H., Alessandrini, S., Kumar, R., & Lin, C.-A. (2020). Estimation of PM2.5 Concentrations in New York State: Understanding the Influence of Vertical Mixing on Surface PM2.5 Using Machine Learning. Atmosphere, 11
21. Imani, M. (2021). Particulate matter (PM2.5 and PM10) generation map using MODIS Level-1 satellite images and deep neural network. Journal of environmental management, 281, 111888-111888
22. Jiang, T., Chen, B., Nie, Z., Ren, Z., Xu, B., & Tang, S. (2021). Estimation of hourly full-coverage PM2.5 concentrations at 1-km resolution in China using a two-stage random forest model. Atmospheric Research, 248
23. Jung, C.-R., Hwang, B.-F., & Chen, W.-T. (2018). Incorporating long-term satellite-based aerosol optical depth, localized land use data, and meteorological variables to estimate ground-level PM2.5 concentrations in Taiwan from 2005 to 2015. Environmental Pollution, 237, 1000-1010
24. Kianian, B., Liu, Y., & Chang, H.H. (2021). Imputing Satellite-Derived Aerosol Optical Depth Using a Multi-Resolution Spatial Model and Random Forest for PM2.5 Prediction. Remote Sensing, 13
25. Kim, S.-M., Yoon, J., Moon, K.-J., Kim, D.-R., Koo, J.-H., Choi, M., Kim, K.N., & Lee, Y.G. (2018). Empirical Estimation and Diurnal Patterns of Surface PM2.5 Concentration in Seoul Using GOCI AOD. Korean Journal of Remote Sensing, 34, 451-463
26. Knibbs, L.D., van Donkelaar, A., Martin, R.V., Bechle, M.J., Brauer, M., Cohen, D.D., Cowie, C.T., Dirgawati, M., Guo, Y., Brauer, M., Cohen, D.D., Cowie, C.T., Dirgawati, M., Guo, Y., Hanigan, I.C., Johnston, F.H., Marks, G.B., Marshall, J.D., Pereira, G., Jalaludin, B., Heyworth, J.S., Morgan, G.G., & Barnett, A.G. (2018). Satellite-Based Land-Use Regression for Continental-Scale Long-Term Ambient PM2.5 Exposure Assessment in Australia. Environmental Science & Technology, 52, 12445-12455
27. Kow, P.-Y., Wang, Y.-S., Zhou, Y., Kao, I.F., Issermann, M., Chang, L.-C., & Chang, F.-J. (2020). Seamless integration of convolutional and back-propagation neural networks for regional multi-step-ahead PM2.5 forecasting. Journal of Cleaner Production, 261
28. Lee, H.J., Chatfield, R.B., & Strawa, A.W. (2016). Enhancing the Applicability of Satellite Remote Sensing for PM2.5 Estimation Using MODIS Deep Blue AOD and Land Use Regression in California, United States. Environmental Science & Technology, 50, 6546-6555
29. Li, H., Yang, Y., Wang, H., Li, B., Wang, P., Li, J., & Liao, H. (2021a). Constructing a spatiotemporally coherent long-term PM2.5 concentration dataset over China during 1980-2019 using a machine learning approach. Science of the Total Environment, 765
30. Li, J., Garshick, E., Hart, J.E., Li, L., Shi, L., Al-Hemoud, A., Huang, S., & Koutrakis, P. (2021b). Estimation of ambient PM2.5 in Iraq and Kuwait from 2001 to 2018 using machine learning and remote sensing. Environment International, 151, 106445-106445
31. Li, L. (2020). A Robust Deep Learning Approach for Spatiotemporal Estimation of Satellite AOD and PM2.5. Remote Sensing, 12
32. Li, L., Girguis, M., Lurmann, F., Pavlovic, N., McClure, C., Franklin, M., Wu, J., Oman, L.D., Breton, C., Gilliland, F., & Habre, R. (2020a). Ensemble-based deep learning for estimating PM2.5 over California with multisource big data including wildfire smoke. Environment International, 145
33. Li, L., Zhang, J., Meng, X., Fang, Y., Ge, Y., Wang, J., Wang, C., Wu, J., & Kan, H. (2018). Estimation of PM2.5 concentrations at a high spatiotemporal resolution using constrained mixed-effect bagging models with MAIAC aerosol optical depth. Remote Sensing of Environment, 217, 573-586
34. Li, S., Zou, B., Fang, X., & Lin, Y. (2020b). Time series modeling of PM2.5 concentrations with residual variance constraint in eastern mainland China during 2013-2017. Science of the Total Environment, 710
35. Li, T., Shen, H., Yuan, Q., & Zhang, L. (2020c). Geographically and temporally weighted neural networks for satellite-based mapping of ground-level PM2.5. Isprs Journal of Photogrammetry and Remote Sensing, 167, 178-188
36. Li, T., Shen, H., Yuan, Q., Zhang, X., & Zhang, L. (2017). Estimating Ground-Level PM2.5 by Fusing Satellite and Station Observations: A Geo-Intelligent Deep Learning Approach. Geophysical Research Letters, 44, 11985-11993

37. Li, X., & Zhang, X. (2019). Predicting ground-level PM2.5 concentrations in the Beijing-Tianjin-Hebei region: A hybrid remote sensing and machine learning approach. Environmental Pollution, 249, 735-749
38. Li, Z., Yim, S.H.-L., & Ho, K.-F. (2020d). High temporal resolution prediction of street-level PM2.5 and NOx concentrations using machine learning approach. Journal of Cleaner Production, 268
39. Liang, F., Xiao, Q., Huang, K., Yang, X., Liu, F., Li, J., Lu, X., Liu, Y., & Gu, D. (2020). The 17-y spatiotemporal trend of PM2.5 and its mortality burden in China. Proceedings of the National Academy of Sciences of the United States of America, 117, 25601-25608
40. Liu, J., Weng, F., & Li, Z. (2019). Satellite-based PM2.5 estimation directly from reflectance at the top of the atmosphere using a machine learning algorithm. Atmospheric Environment, 208, 113-122
41. Lu, J., Zhang, Y., Chen, M., Wang, L., Zhao, S., Pu, X., & Chen, X. (2021). Estimation of monthly 1 km resolution PM2.5 concentrations using a random forest model over "2+26" cities, China. Urban Climate, 35
42. Luo, Y., Teng, M., Yang, K., Zhu, Y., Zhou, X., Zhang, M., & Shi, Y. (2019). Research on PM2.5 estimation and prediction method and changing characteristics analysis under long temporal and large spatial scale - A case study in China typical regions. Science of the Total Environment, 696
43. Lv, B., Hu, Y., Chang, H.H., Russell, A.G., Cai, J., Xu, B., & Bai, Y. (2017). Daily estimation of ground-level PM2.5 concentrations at 4 km resolution over Beijing-Tianjin-Hebei by fusing MODIS AOD and ground observations. Science of the Total Environment, 580, 235-244
44. Lyu, B., Hu, Y., Zhang, W., Du, Y., Luo, B., Sun, X., Sun, Z., Deng, Z., Wang, X., Liu, J., Wang, X., & Russell, A.G. (2019). Fusion Method Combining Ground-Level Observations with Chemical Transport Model Predictions Using an Ensemble Deep Learning Framework: Application in China to Estimate Spatiotemporally-Resolved PM2.5 Exposure Fields in 2014-2017. Environmental Science & Technology, 53, 7306-7315
45. Ma, J., Cheng, J.C.P., Lin, C., Tan, Y., & Zhang, J. (2019). Improving air quality prediction accuracy at larger temporal resolutions using deep learning and transfer learning techniques. Atmospheric Environment, 214
46. Ma, Z., Liu, Y., Zhao, Q., Liu, M., Zhou, Y., & Bi, J. (2016). Satellite-derived high resolution PM2.5 concentrations in Yangtze River Delta Region of China using improved linear mixed effects model. Atmospheric Environment, 133, 156-164
47. Nabavi, S.O., Haimberger, L., & Abbasi, E. (2019). Assessing PM2.5 concentrations in Tehran, Iran, from space using MAIAC, deep blue, and dark target AOD and machine learning algorithms. Atmospheric Pollution Research, 10, 889-903
48. Nguyen, T.T.N., Bui, H.Q., Pham, H.V., Luu, H.V., Man, C.D., Pham, H.N., Le, H.T., & Nguyen, T.T. (2015). Particulate matter concentration mapping from MODIS satellite data: a Vietnamese case study. Environmental Research Letters, 10
49. Ni, X., Cao, C., Zhou, Y., Cui, X., & Singh, R.P. (2018). Spatio-Temporal Pattern Estimation of PM2.5 in Beijing-Tianjin-Hebei Region Based on MODIS AOD and Meteorological Data Using the Back Propagation Neural Network. Atmosphere, 9
50. Park, S., Lee, J., Im, J., Song, C.-K., Choi, M., Kim, J., Lee, S., Park, R., Kim, S.-M., Yoon, J., Lee, D.-W., & Quackenbush, L.J. (2020a). Estimation of spatially continuous daytime particulate matter concentrations under all sky conditions through the synergistic use of satellite-based AOD and numerical models. Science of the Total Environment, 713
51. Park, S., Shin, M., Im, J., Song, C.-K., Choi, M., Kim, J., Lee, S., Park, R., Kim, J., Lee, D.-W., & Kim, S.-K. (2019). Estimation of ground-level particulate matter concentrations through the synergistic use of satellite observations and process-based models over South Korea. Atmospheric Chemistry and Physics, 19, 1097-1113
52. Park, Y., Kwon, B., Heo, J., Hu, X., Liu, Y., & Moon, T. (2020b). Estimating PM2.5 concentration of the conterminous United States via interpretable convolutional neural networks. Environmental Pollution, 256
53. Pu, Q., & Yoo, E.-H. (2021). Ground PM2.5 prediction using imputed MAIAC AOD with uncertainty quantification. Environmental pollution (Barking, Essex : 1987), 274, 116574-116574
54. Ren, X., Mi, Z., & Georgopoulos, P.G. (2020). Comparison of Machine Learning and Land Use Regression for fine scale spatiotemporal estimation of ambient air pollution: Modeling ozone concentrations across the contiguous United States. Environment International, 142
55. Schneider, R., Vicedo-Cabrera, A.M., Sera, F., Masselot, P., Stafoggia, M., de Hoogh, K., Kloog, I., Reis, S., Vieno, M., & Gasparrini, A. (2020). A Satellite-Based Spatio-Temporal Machine Learning Model to Reconstruct Daily PM2.5 Concentrations across Great Britain. Remote Sensing, 12
56. Song, W., Jia, H., Huang, J., & Zhang, Y. (2014). A satellite-based geographically weighted regression model for regional PM2.5 estimation over the Pearl River Delta region in China. Remote Sensing of Environment, 154, 1-7
57. Stafoggia, M., Bellander, T., Bucci, S., Davoli, M., de Hoogh, K., de'Donato, F., Gariazzo, C., Lyapustin, A., Michelozzi, P., Renzi, M., Scortichini, M., Shtein, A., Viegi, G., Kloog, I., & Schwartz, J. (2019). Estimation of daily PM10 and PM2.5 concentrations in Italy, 2013-2015, using a spatiotemporal land-use random-forest model. Environment International, 124, 170-179
58. Sun, Y., Zeng, Q., Geng, B., Lin, X., Sude, B., & Chen, L. (2019). Deep Learning Architecture for Estimating Hourly Ground-Level PM2.5 Using Satellite Remote Sensing. Ieee Geoscience and Remote Sensing Letters, 16, 1343-1347
59. Tang, D., Liu, D., Tang, Y., Seyler, B.C., Deng, X., & Zhan, Y. (2019). Comparison of GOCI and Himawari-8 aerosol optical depth for deriving full-coverage hourly PM2.5 across the Yangtze River Delta. Atmospheric Environment, 217
60. Tian, H., Zhao, Y., Luo, M., He, Q., Han, Y., & Zeng, Z. (2021). Estimating PM2.5 from multisource data: A comparison of different machine learning models in the Pearl River Delta of China. Urban Climate, 35
61. Tong, W., Li, L., Zhou, X., Hamilton, A., & Zhang, K. (2019). Deep learning PM2.5 concentrations with bidirectional LSTM RNN. Air Quality Atmosphere and Health, 12, 411-423

62. van Donkelaar, A., Martin, R.V., Spurr, R.J.D., & Burnett, R.T. (2015). High-Resolution Satellite-Derived PM2.5 from Optimal Estimation and Geographically Weighted Regression over North America. Environmental Science & Technology, 49, 10482-10491
63. Wang, B., Yuan, Q., Yang, Q., Zhu, L., Li, T., & Zhang, L. (2021). Estimate hourly PM2.5 concentrations from Himawari-8 TOA reflectance directly using geo-intelligent long short-term memory network. Environmental pollution (Barking, Essex : 1987), 271, 116327-116327
64. Wang, Q., Zeng, Q., Tao, J., Sun, L., Zhang, L., Gu, T., Wang, Z., & Chen, L. (2019). Estimating PM2.5 Concentrations Based on MODIS AOD and NAQPMS Data over Beijing-Tianjin-Hebei. Sensors, 19
65. Wang, W., Mao, F., Du, L., Pan, Z., Gong, W., & Fang, S. (2017). Deriving Hourly PM2.5 Concentrations from Himawari-8 AODs over Beijing-Tianjin-Hebei in China. Remote Sensing, 9
66. Wang, X., & Sun, W. (2019). Meteorological parameters and gaseous pollutant concentrations as predictors of daily continuous PM2.5 concentrations using deep neural network in Beijing-Tianjin-Hebei, China. Atmospheric Environment, 211, 128-137
67. Wei, J., Huang, W., Li, Z., Xue, W., Peng, Y., Sun, L., & Cribb, M. (2019). Estimating 1-km-resolution PM2.5 concentrations across China using the space-time random forest approach. Remote Sensing of Environment, 231
68. Wei, J., Li, Z., Cribb, M., Huang, W., Xue, W., Sun, L., Guo, J., Peng, Y., Li, J., Lyapustin, A., Liu, L., Wu, H., & Song, Y. (2020). Improved 1 km resolution PM2.5 estimates across China using enhanced space-time extremely randomized trees. Atmospheric Chemistry and Physics, 20, 3273-3289
69. Wei, J., Li, Z., Lyapustin, A., Sun, L., Peng, Y., Xue, W., Su, T., & Cribb, M. (2021). Reconstructing 1-km-resolution high-quality PM2.5 data records from 2000 to 2018 in China: spatiotemporal variations and policy implications. Remote Sensing of Environment, 252
70. Wu, J., Yao, F., Li, W., & Si, M. (2016). VIIRS-based remote sensing estimation of ground-level PM2.5 concentrations in Beijing-Tianjin-Hebei: A spatiotemporal statistical model. Remote Sensing of Environment, 184, 316-328
71. Xiao, F., Yang, M., Fan, H., Fan, G., & Al-qaness, M.A.A. (2020). An improved deep learning model for predicting daily PM2.5 concentration. Scientific Reports, 10
72. Xiao, L., Lang, Y., & Christakos, G. (2018). High-resolution spatiotemporal mapping of PM2.5 concentrations at Mainland China using a combined BME-GWR technique. Atmospheric Environment, 173, 295-305
73. Xie, Y., Wang, Y., Zhang, K., Dong, W., Lv, B., & Bai, Y. (2015). Daily Estimation of Ground-Level PM2.5 Concentrations over Beijing Using 3 km Resolution MODIS AOD. Environmental Science & Technology, 49, 12280-12288
74. Xing, H., Wang, G., Liu, C., & Suo, M. (2021). PM2.5 concentration modeling and prediction by using temperature-based deep belief network. Neural Networks, 133, 157-165
75. Xu, X., Tong, T., Zhang, W., & Meng, L. (2020). Fine-grained prediction of PM2.5 concentration based on multisource data and deep learning. Atmospheric Pollution Research, 11, 1728-1737
76. Xu, X., & Zhang, C. (2020). Estimation of ground-level PM(2.5)concentration using MODIS AOD and corrected regression model over Beijing, China. Plos One, 15
77. Xu, Y., Ho, H.C., Wong, M.S., Deng, C., Shi, Y., Chan, T.-C., & Knudby, A. (2018). Evaluation of machine learning techniques with multiple remote sensing datasets in estimating monthly concentrations of ground-level PM2.5. Environmental Pollution, 242, 1417-1426
78. Xue, W., Wei, J., Zhang, J., Sun, L., Che, Y., Yuan, M., & Hu, X. (2021a). Inferring Near-Surface PM2.5 Concentrations from the VIIRS Deep Blue Aerosol Product in China: A Spatiotemporally Weighted Random Forest Model. Remote Sensing, 13
79. Xue, W., Zhang, J., Zhong, C., Li, X., & Wei, J. (2021b). Spatiotemporal PM2.5 variations and its response to the industrial structure from 2000 to 2018 in the Beijing-Tianjin-Hebei region. Journal of Cleaner Production, 279
80. Xue, Y., Li, Y., Guang, J., Tugui, A., She, L., Qin, K., Fan, C., Che, Y., Xie, Y., Wen, Y., & Wang, Z. (2020). Hourly PM2.5 Estimation over Central and Eastern China Based on Himawari-8 Data. Remote Sensing, 12
81. Yan, X., Zang, Z., Jiang, Y., Shi, W., Guo, Y., Li, D., Zhao, C., & Husi, L. (2021). A Spatial-Temporal Interpretable Deep Learning Model for improving interpretability and predictive accuracy of satellite-based PM2.5. Environmental pollution (Barking, Essex : 1987), 273, 116459-116459
82. Yang, L., Xu, H., & Jin, Z. (2018a). Estimating spatial variability of ground-level PM2.5 based on a satellite-derived aerosol optical depth product: Fuzhou, China. Atmospheric Pollution Research, 9, 1194-1203
83. Yang, L., Xu, H., & Jin, Z. (2019). Estimating ground-level PM2.5 over a coastal region of China using satellite AOD and a combined model. Journal of Cleaner Production, 227, 472-482
84. Yang, Q., Yuan, Q., Li, T., & Yue, L. (2020). Mapping PM2.5 concentration at high resolution using a cascade random forest based downscaling model: Evaluation and application. Journal of Cleaner Production, 277
85. Yang, S., Wu, H., Chen, J., Lin, X., & Lu, T. (2018b). Optimization of PM2.5 Estimation Using Landscape Pattern Information and Land Use Regression Model in Zhejiang, China. Atmosphere, 9
86. You, W., Zang, Z., Zhang, L., Li, Y., Pan, X., & Wang, W. (2016a). National-Scale Estimates of Ground-Level PM2.5 Concentration in China Using Geographically Weighted Regression Based on 3 km Resolution MODIS AOD. Remote Sensing, 8
87. You, W., Zang, Z., Zhang, L., Li, Y., & Wang, W. (2016b). Estimating national-scale ground-level PM25 concentration in China using geographically weighted regression based on MODIS and MISR AOD. Environmental Science and Pollution Research, 23, 8327-8338

88. Zhai, L., Li, S., Zou, B., Sang, H., Fang, X., & Xu, S. (2018). An improved geographically weighted regression model for PM2.5 concentration estimation in large areas. Atmospheric Environment, 181, 145-154
89. Zhan, Y., Luo, Y., Deng, X., Chen, H., Grieneisen, M.L., Shen, X., Zhu, L., & Zhang, M. (2017). Spatiotemporal prediction of continuous daily PM2.5 concentrations across China using a spatially explicit machine learning algorithm. Atmospheric Environment, 155, 129-139
90. Zhang, Q., Wu, S., Wang, X., Sun, B., & Liu, H. (2020a). A PM2.5 concentration prediction model based on multi-task deep learning for intensive air quality monitoring stations. Journal of Cleaner Production, 275
91. Zhang, R., Di, B., Luo, Y., Deng, X., Grieneisen, M.L., Wang, Z., Yao, G., & Zhan, Y. (2018a). A nonparametric approach to filling gaps in satellite-retrieved aerosol optical depth for estimating ambient PM2.5 levels. Environmental Pollution, 243, 998-1007
92. Zhang, T., He, W., Zheng, H., Cui, Y., Song, H., & Fu, S. (2021). Satellite-based ground PM2.5 estimation using a gradient boosting decision tree. Chemosphere, 268, 128801-128801
93. Zhang, T., Liu, G., Zhu, Z., Gong, W., Ji, Y., & Huang, Y. (2016). Real-Time Estimation of Satellite-Derived PM2.5 Based on a Semi-Physical Geographically Weighted Regression Model. International Journal of Environmental Research and Public Health, 13
94. Zhang, T., Zhu, Z., Gong, W., Zhu, Z., Sun, K., Wang, L., Huang, Y., Mao, F., Shen, H., Li, Z., & Xu, K. (2018b). Estimation of ultrahigh resolution PM2.5 concentrations in urban areas using 160 m Gaofen-1 AOD retrievals. Remote Sensing of Environment, 216, 91-104
95. Zhang, X., & Hu, H. (2017). Improving Satellite-Driven PM2.5 Models with VIIRS Nighttime Light Data in the Beijing-Tianjin-Hebei Region, China. Remote Sensing, 9
96. Zhang, Y., Wang, W., Ma, Y., Wu, L., Xu, W., & Li, J. (2020b). Improvement in hourly PM2.5 estimations for the Beijing-Tianjin-Hebei region by introducing an aerosol modeling product from MASINGAR. Environmental Pollution, 264
97. Zhao, C., Wang, Q., Ban, J., Liu, Z., Zhang, Y., Ma, R., Li, S., & Li, T. (2020). Estimating the daily PM2.5 concentration in the Beijing-Tianjin-Hebei region using a random forest model with a 0.01 degrees x 0.01 degrees spatial resolution. Environment International, 134
98. Zheng, T., Bergin, M.H., Hu, S., Miller, J., & Carlson, D.E. (2020). Estimating ground-level PM2.5 using micro-satellite images by a convolutional neural network and random forest approach. Atmospheric Environment, 230
99. Zhou, W., Wu, X., Ding, S., Ji, X., & Pan, W. (2021). Predictions and mitigation strategies of PM2.5 concentration in the Yangtze River Delta of China based on a novel nonlinear seasonal grey model. Environmental pollution (Barking, Essex : 1987), 276, 116614-116614
100. Zou, B., Chen, J., Zhai, L., Fang, X., & Zheng, Z. (2017). Satellite Based Mapping of Ground PM2.5 Concentration Using Generalized Additive Modeling. Remote Sensing, 9
101. Zou, B., Pu, Q., Bilal, M., Weng, Q., Zhai, L., & Nichol, J.E. (2016). High-Resolution Satellite Mapping of Fine Particulates Based on Geographically Weighted Regression. Ieee Geoscience and Remote Sensing Letters, 13, 495-499